CRISPR-based ultrasensitive array for early diagnosis of Alzheimer's disease by detecting multiple plasma biomarkers

Liding Zhang[1#], Changwen Yang[2#], Xuewei Du[1], Hui Gong[2,3], Yin Han[1,4,5*], Qingming Luo[1], Haiming Luo[1,2,3*]

[1]Key Laboratory of Biomedical Engineering of Hainan Province, School of Biomedical Engineering, Hainan University, 570228, Haikou, China

[2]Britton Chance Center for Biomedical Photonics, Wuhan National Laboratory for Optoelectronics, Huazhong University of Science and Technology, 430070, Wuhan, China

[3]HUST-Suzhou Institute for Brainsmatics, Jiangsu Industrial Technology Research Institute (JITRI), 215123, Suzhou, China

[4]Department of Neurology, Xuanwu Hospital of Capital Medical University, 100053, Beijing, China

[5]Center of Alzheimer's Disease, Beijing Institute for Brain Disorders, 100053, Beijing, China

*Corresponding author: Haiming Luo, hemluo@hainanu.edu.cn; Yin Han, hanying@xwh.ccmu.edu.cn

Key Laboratory of Biomedical Engineering of Hainan Province, School of Biomedical Engineering, Hainan University, 570228, Haikou, China;

Table of Contents

Supplementary Table 11 Comparison of AUC values, sensitivity, specificity, precision, and accuracy of UCMDA and Sioma using the predictor of $A\beta_{42}$, $A\beta_{42}/A\beta_{40}$, or p-tau^{181} in distinguishing between non-NCs and NCs

Supplementary Table 12 The AUC value, sensitivity, specificity, precision, and accuracy of different algorithms using the predictor of composite biomarkers detected by UCMDA in distinguishing between AD patients and NCs

Supplementary Table 13 The AUC value, sensitivity, specificity, precision, and accuracy of different algorithms using the predictor of composite biomarkers detected by UCMDA in distinguishing between AD-related MCI and NCs

Supplementary Table S14 The AUC value, sensitivity, specificity, precision, and accuracy of different algorithms using the predictor of composite biomarkers detected by UCMDA in distinguish between non-NCs and NCs

Supplementary Table S15 Details of antibodies used in UCMDA platform

Supplementary Table S16 The sequence of synthesized peptides used in this study

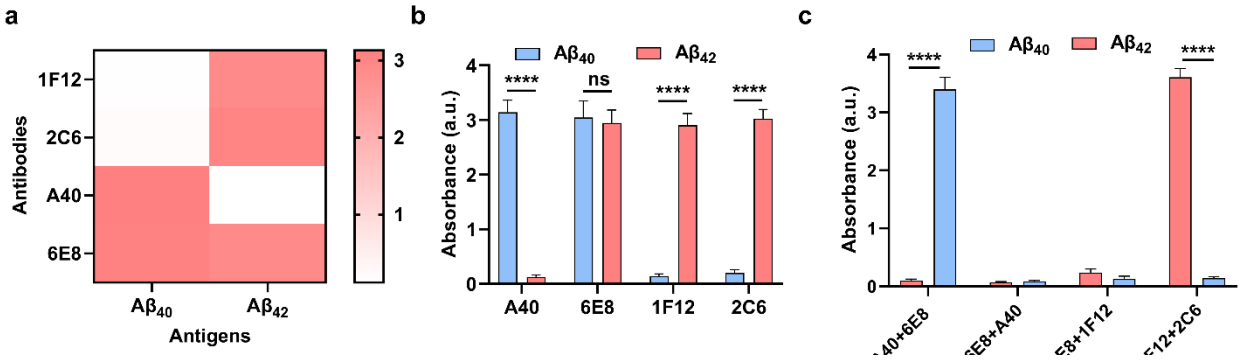

Supplementary Fig. 1 | Characterization of anti-Aβ conformation-dependent antibodies. a, b Heat map **(a)** and quantitative analysis **(b)** of the selectivity of different antibodies for $A\beta_{42}$ and $A\beta_{40}$. **c** Screening of the best antibody pairs for detecting $A\beta_{42}$ and $A\beta_{40}$. Data are presented as mean or mean ± s.d. (n = 4, ****$p < 0.0001$). Two-way ANOVA was used for statistical analysis.

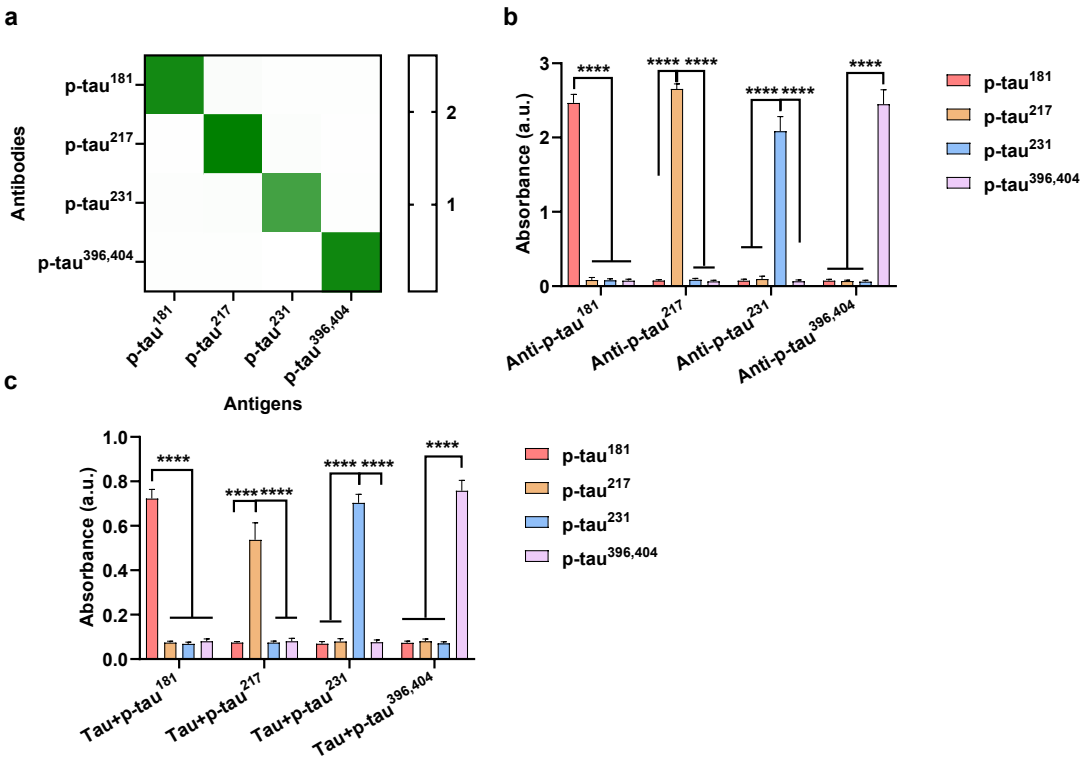

Supplementary Fig. 2 | Characterization of phosphorylated tau selective antibodies. a, b Heat map **(a)** and quantitative analysis **(b)** of antibody selectivity for p-tau^{181}, p-tau^{217}, p-tau^{231}, and p-tau^{396,404}. **c,** Specificity of antibody pairs for detecting p-tau^{181}, p-tau^{217}, p-tau^{231}, and p-tau^{396,404}. Data are presented as mean or mean ± s.d. (n = 4, ****p < 0.0001). Two-way ANOVA was used for statistical analysis.

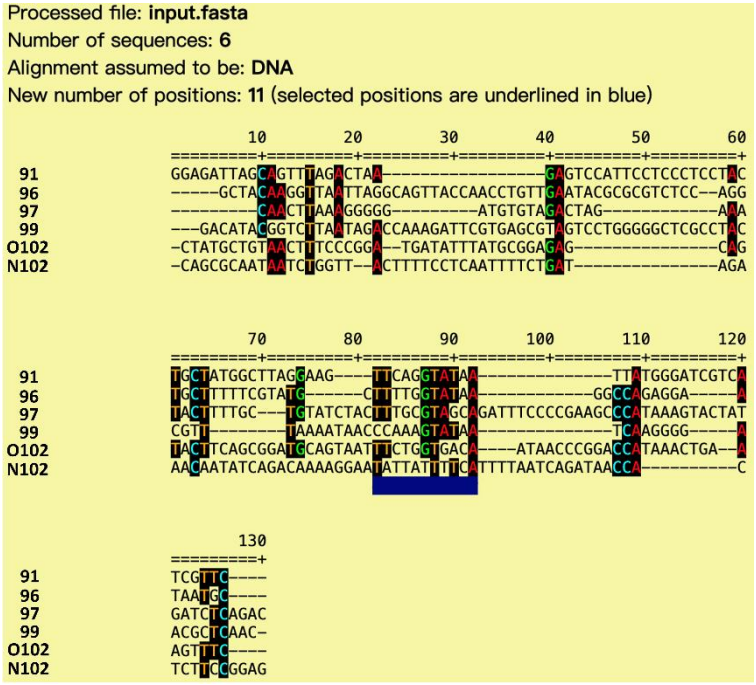

Supplementary Fig. 3 | Sequence specificity analysis between different ssDNA.

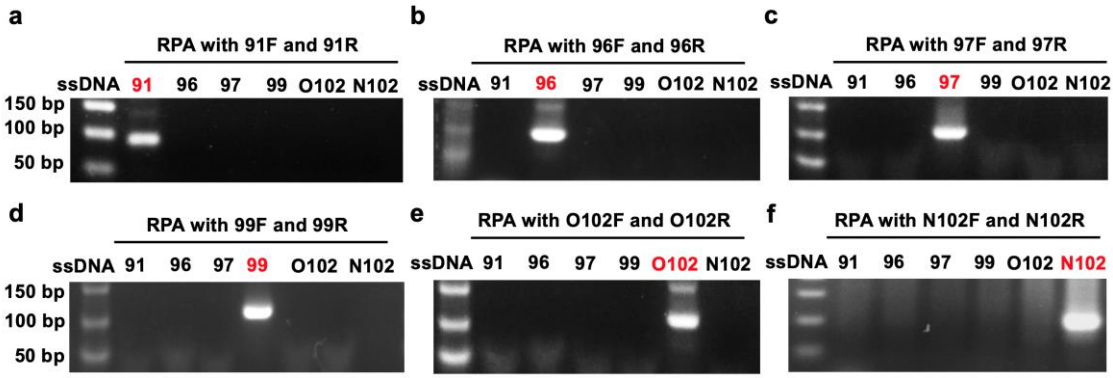

Supplementary Fig. 4 | Selectivity of RPA primers. a-f Agarose gel images of RPA products for evaluating the selectivity of RPA primers for ssDNA 91 **(a)**, ssDNA 96 **(b)**, ssDNA 97 **(c)**, ssDNA 99 **(d)**, ssDNA O102 **(e)**, or ssDNA N102 **(f)** in the presence of six ssDNA, including ssDNA 96, ssDNA 97, ssDNA 99, ssDNA O102, and ssDNA N102.

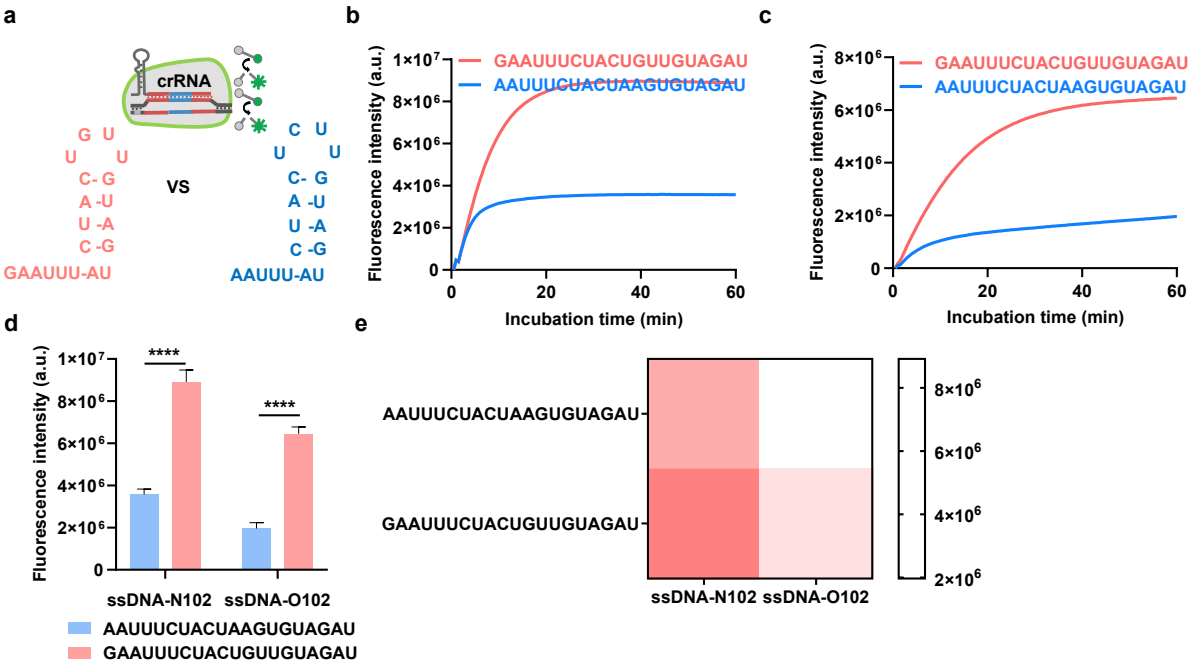

Supplementary Fig. 5 | Optimization of crRNA sequences. a Scaffold sequences of two crRNAs**. b-e** Kinetic curves of CRISPR-Cas12a for the detection of dsDNA-O102 and dsDNA-N102 in the presence of crRNA (GAAUUUCUACUGUUGUAGAU) **(b)** or crRNA (AAUUUCUACUAAGUGUAGAU) **(c)**. Data are presented as mean. (n = 3). Quantification **(d)** and heat map **(e)** for the analysis of the difference in fluorescence intensity between the two crRNAs. Data are presented as mean or mean ± s.d. (n = 3, ****$p < 0.0001$). Two-way ANOVA was used for statistical analysis.

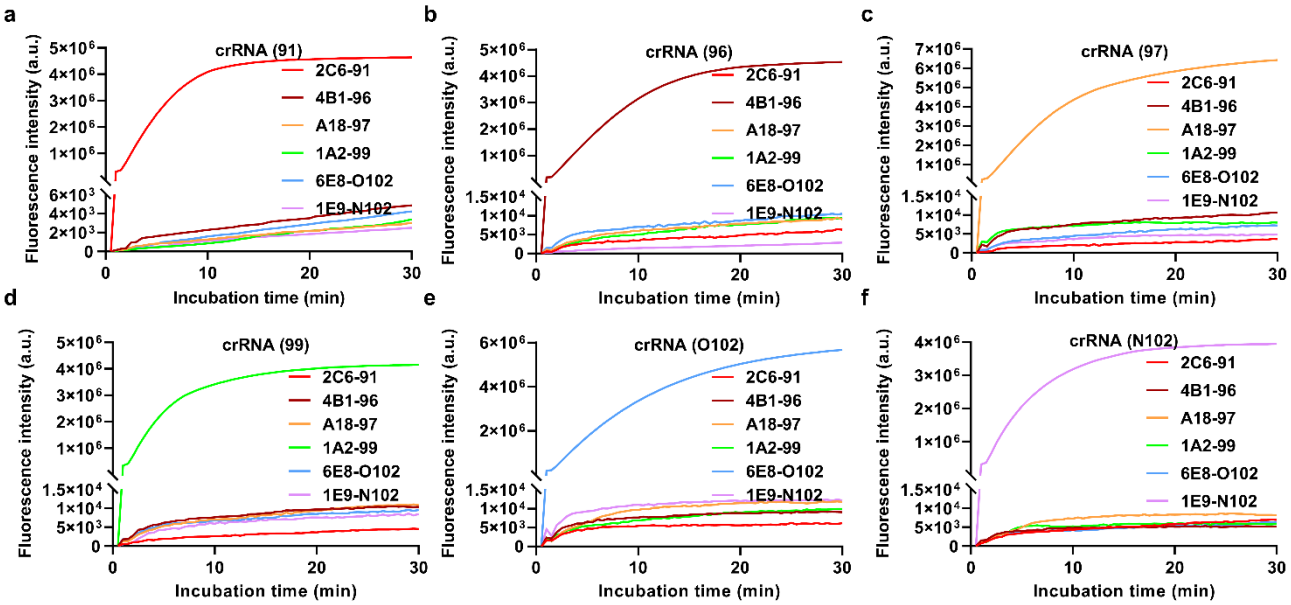

Supplementary Fig. 6 | Evaluation of crRNA selectivity. a-f Kinetic curves of crRNA 91 **(a)**, crRNA 96 **(b)**, crRNA 97 **(c)**, crRNA 99 **(d)**, crRNA O102 **(e)**, and crRNA N102 **(f)** for the detection of six different RPA products in the presence of 2C6-ssDNA 91, 4B1-ssDNA 96, A18-ssDNA 97, 1A2-ssDNA 99, 6E8-ssDNA O102, or 1E9-ssDNA N102. Data are presented as mean (n = 3).

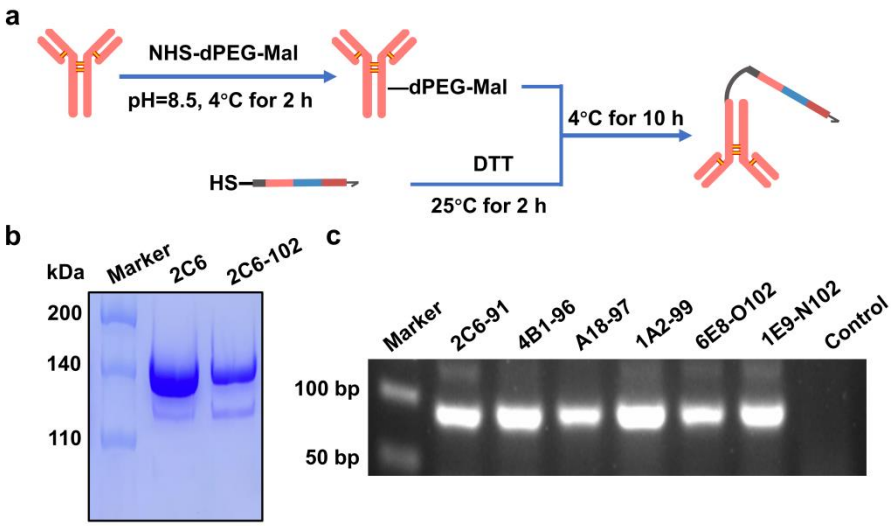

Supplementary Fig. 7 | Synthesis and characterization of antibody-ssDNA. a Flow chart of antibody-ssDNA synthesis. **b** Denaturing non-reducing PAGE gel image of antibody-ssDNA. **c** Agarose gel images of PCR products using 2C6-ssDNA 91, 4B1-ssDNA 96, A18-ssDNA 97, 1A2-ssDNA 99, 6E8-ssDNA O102, and 1E9-ssDNA N102 as templates, respectively.

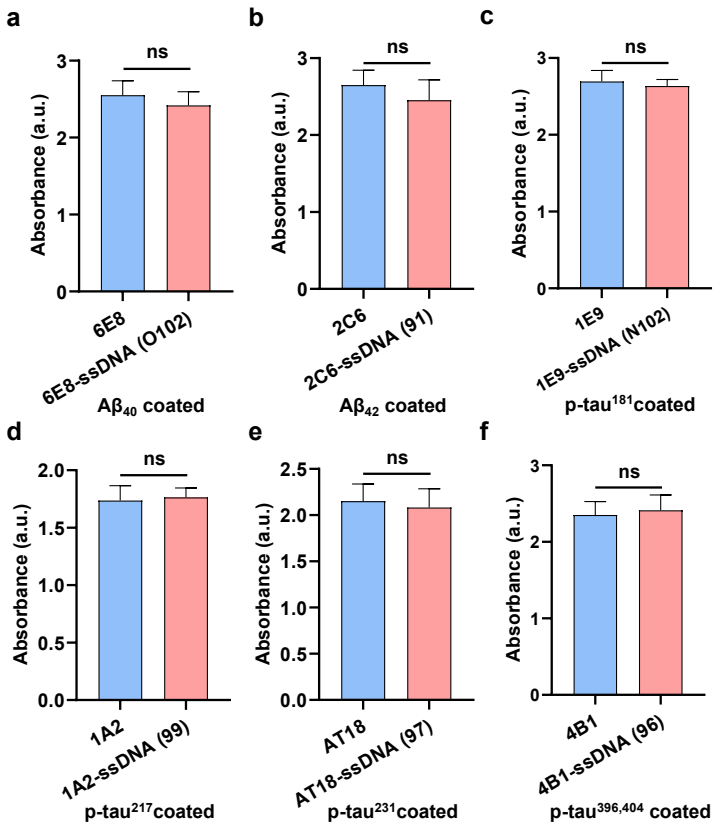

Supplementary Fig. 8 | Evaluation of the biological activity of antibody-ssDNA. a-f ELISA analysis of the biological activities of 2C6-ssDNA 91, 4B1-ssDNA 96, A18-ssDNA 97, 1A2-ssDNA 99, 6E8-ssDNA O102, and 1E9-ssDNA N102 against $A\beta_{40}$ **(a)**, $A\beta_{42}$ **(b)**, p-tau^{181} **(c)**, p-tau^{217} **(d)**, p-tau^{231} **(e)**, and p-tau^{396,404} **(f)**. Data are presented as mean ± s.d. (n = 3). Student's t-test was used for statistical analysis.

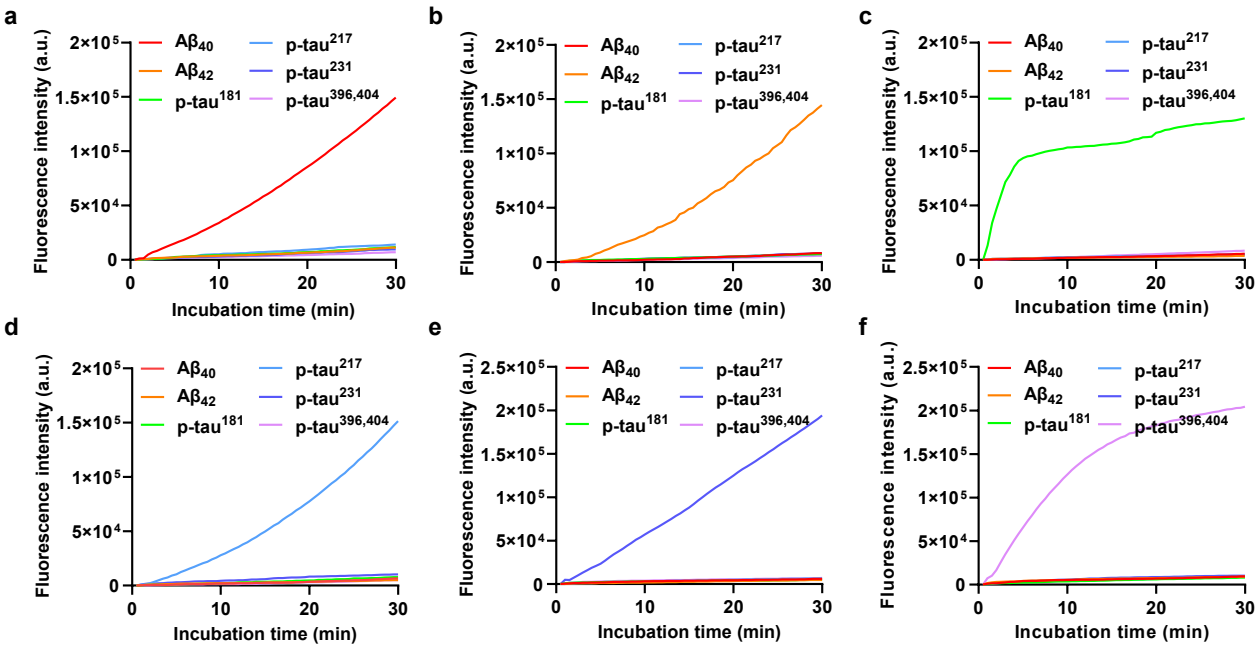

Supplementary Fig. 9 | Specificity of UCMDA. a-f Kinetic curves of UCMDA for the detection of $A\beta_{40}$ **(a)**, **$A\beta_{42}$ (b)**, p-tau^{181} **(c)**, p-tau^{217} **(d)**, p-tau^{231} **(e)**, and p-tau^{396,404} **(f)**. Data are presented as mean (n = 3).

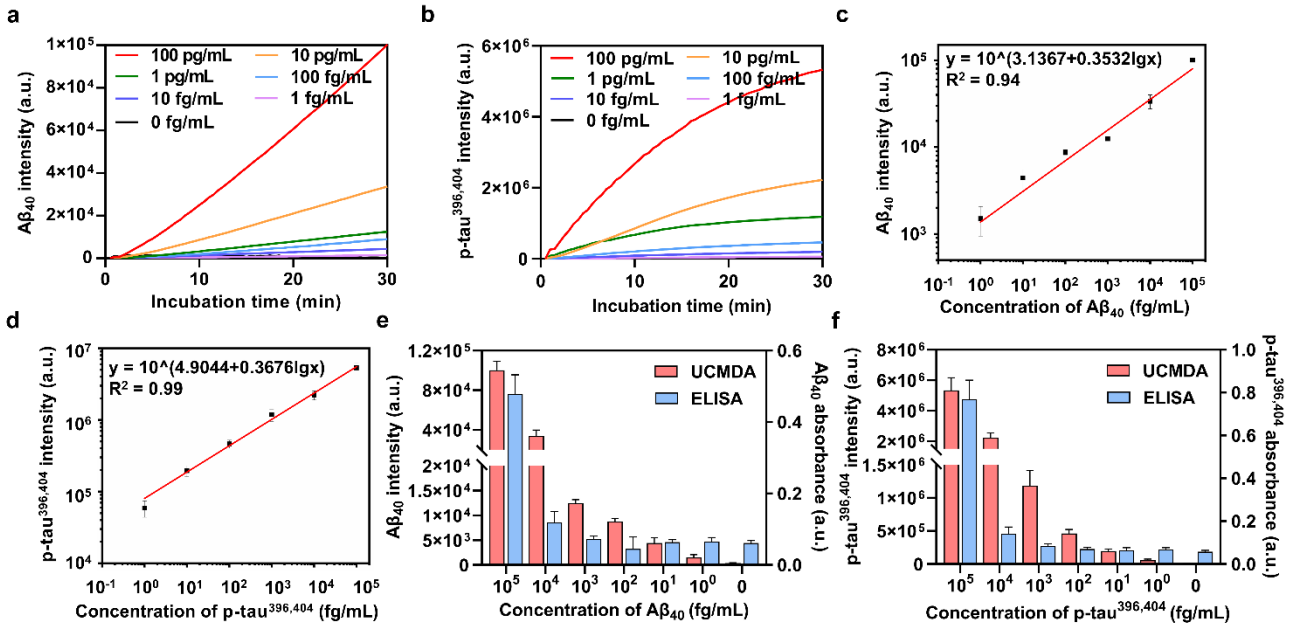

Supplementary Fig. 10 | Sensitivity of UCMDA in standard peptide solutions. a, b Kinetic curves of UCMDA system of different concentrations of Aβ$_{40}$ **(a)** and p-tau^{396,404} **(b)** peptides diluted in TBS buffer. **c, d** Calibration curves for the detection of Aβ$_{40}$ **(c)** and p-tau^{396,404} **(d)** peptide in the range of 1 fg/mL to 100 pg/mL. **e, f** Signals of UCMDA and ELISA detection of different concentrations of Aβ$_{40}$ **(e)** and p-tau^{396,404} **(f)** peptide. Data are presented as mean or mean ± s.d. (n = 3).

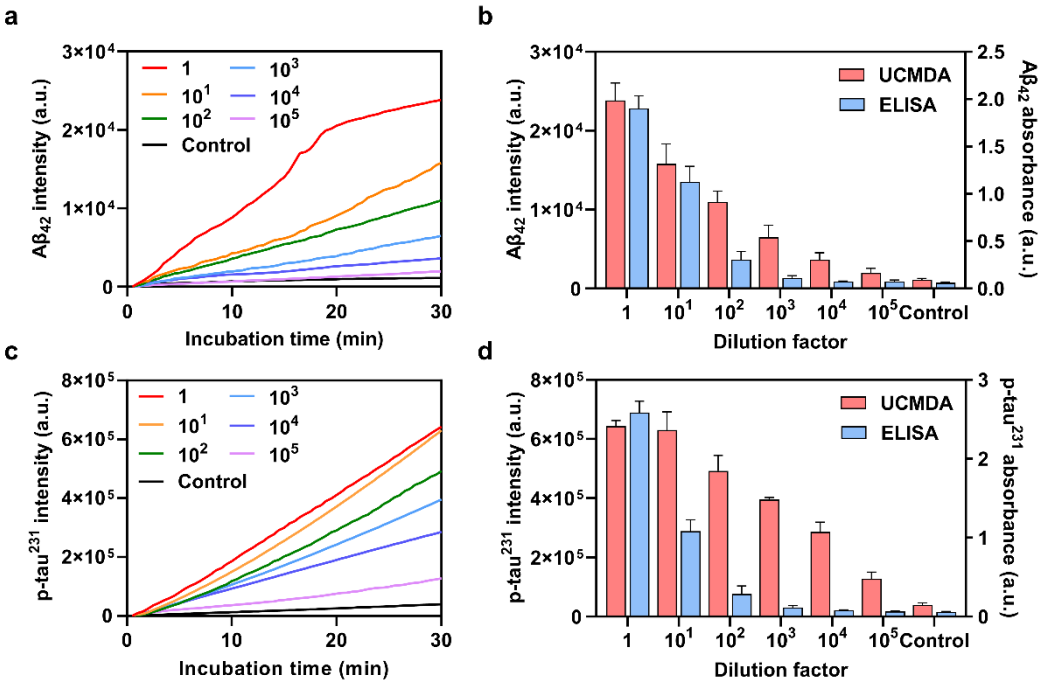

Supplementary Fig. 11 | Sensitivity of UCMDA in the plasma of transgenic mice. a, c Kinetic curves of UCMDA system for detecting Aβ$_{42}$ **(a)** in 5×FAD and p-tau^{231} **(c)** in htau mice plasma at dilutions ranging from 1 to 100,000. **b, d** Signals of Aβ$_{42}$ **(b)** and p-tau^{231} **(d)** detected by UCMDA and ELISA at different dilution ratios. Data are presented as mean or mean ± s.d. (n = 3).

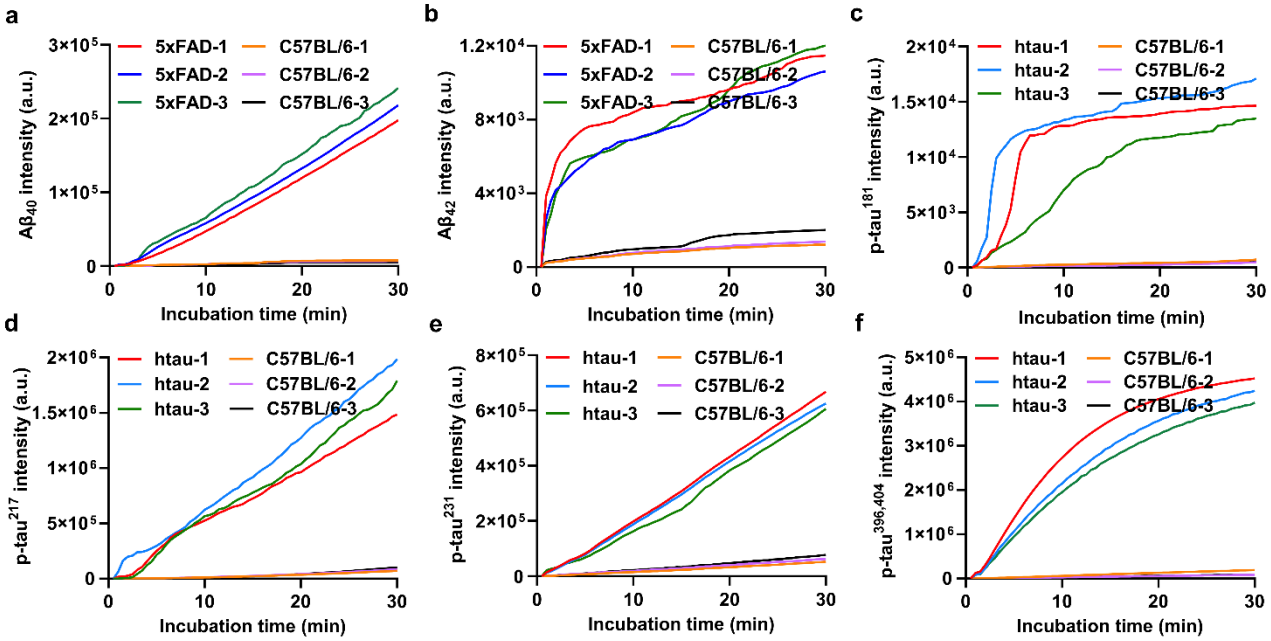

Supplementary Fig. 12 | Kinetic curves of UCMDA for detecting different Aβ and p-tau. a-f Kinetic curves of UCMDA for the detection of $A\beta_{40}$ **(a)**, $A\beta_{42}$ **(b)**, p-tau^{181} **(c)**, p-tau^{217} **(d)**, p-tau^{231} **(e)**, and p-tau^{396,404} **(f)** in plasma samples of AD transgenic mice or C57BL/6 mice.

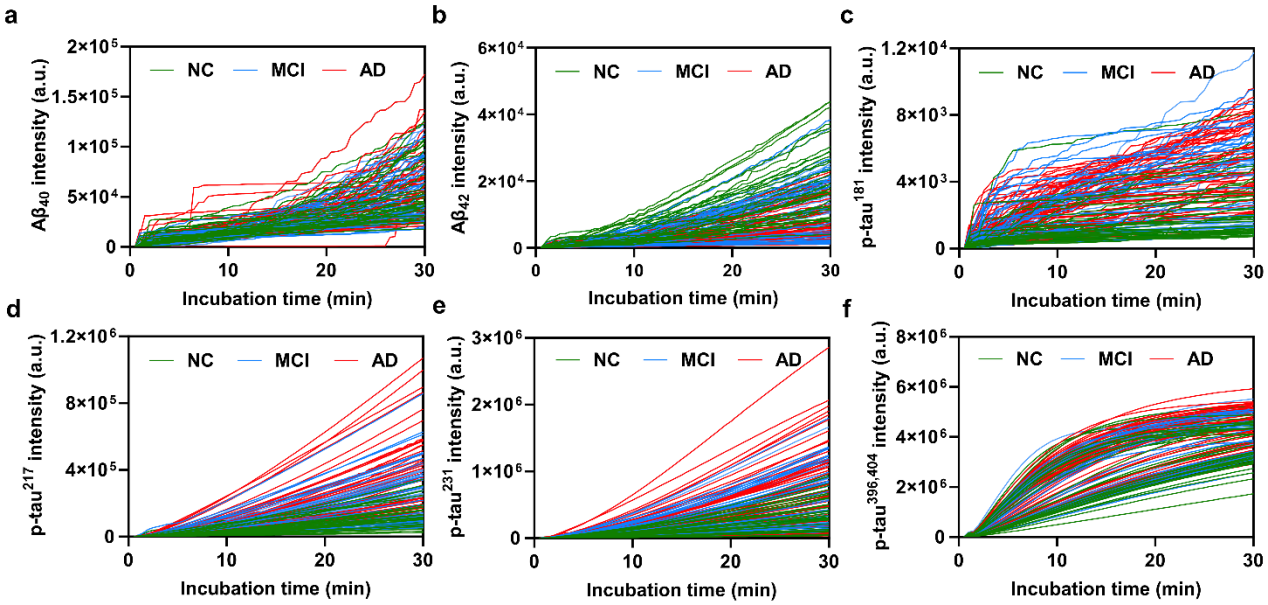

Supplementary Fig. 13 | Clinical validation of UCMDA. a-f Kinetic curves of UCMDA for detecting $A\beta_{40}$ **(a)**, $A\beta_{42}$ **(b)**, p-tau^{181} **(c)**, p-tau^{217} **(d)**, p-tau^{231} **(e)**, and p-tau^{396,404} **(f)** in plasma of patients with AD (n = 56), individuals with AD-related MCI (n = 52), and NCs (n = 47).

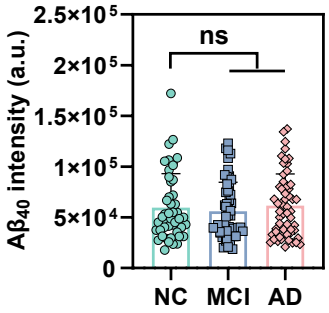

Supplementary Fig. 14 | The fluorescence intensity of Aβ40 in clinical samples. Box plots showing the endpoint fluorescence intensity of Aβ40 in plasma of patients with AD (n = 56), individuals with AD-related MCI (n = 52), and NCs (n = 47). One-way ANOVA was used for statistical analysis.

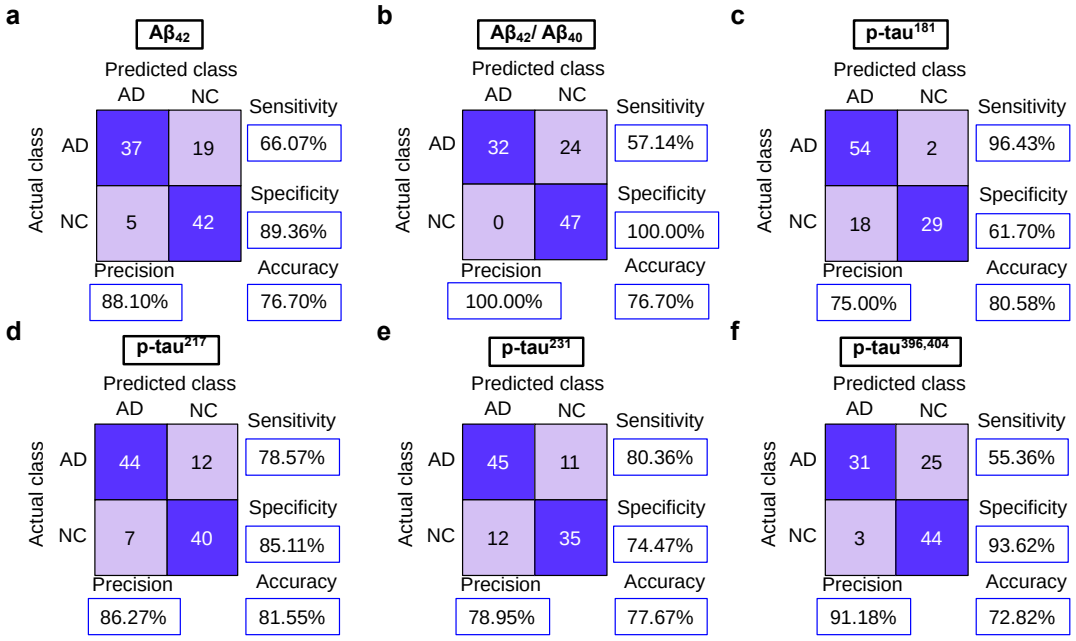

Supplementary Fig. 15 | Performance of UCMDA using the single biomarker in distinguishing AD from NCs. a-f Sensitivity, specificity, precision, and accuracy of ROC analysis based on UCMDA using the predictor of $A\beta_{42}$ **(a)**, $A\beta_{42}/A\beta_{40}$ ratio **(b)**, p-tau^{181} **(c)**, p-tau^{217} **(d)**, p-tau^{231} **(e)**, or p-tau^{396,404} detected by UCMDA **(f)** in distinguishing patients with AD (n = 56) from NCs (n = 47).

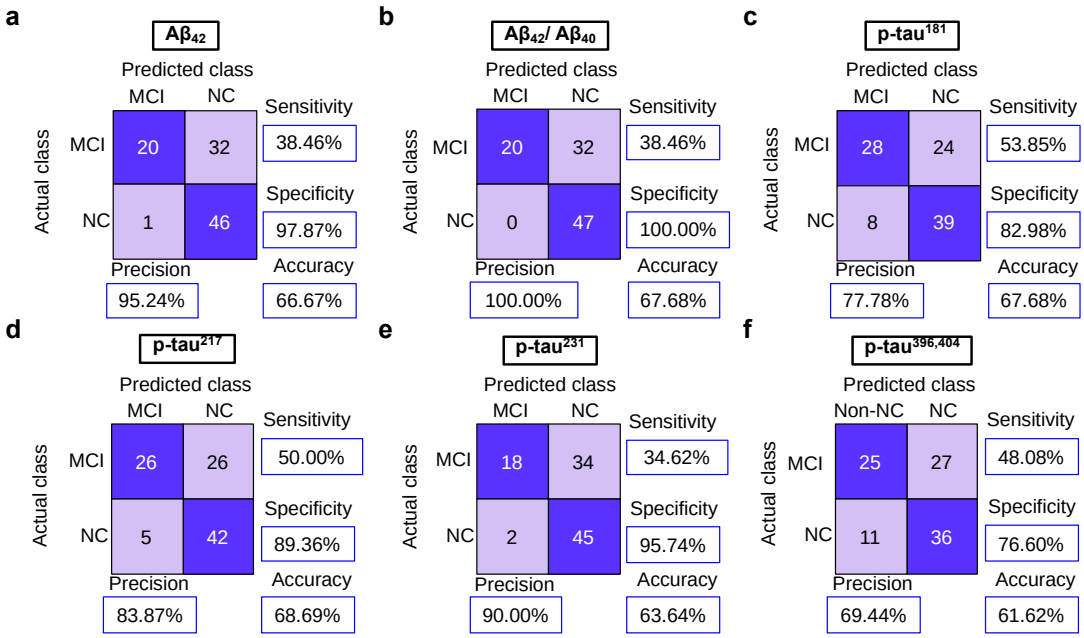

Supplementary Fig. 16 | Performance of UCMDA using the single biomarker in distinguishing AD-related MCI from NCs. a-f Sensitivity, specificity, precision, and accuracy of ROC analysis using the predictor of $A\beta_{42}$ **(a)**, $A\beta_{42}/A\beta_{40}$ ratio **(b)**, p-tau^{181} **(c)**, p-tau^{217} **(d)**, p-tau^{231} **(e)**, or p-tau^{396,404} detected by UCMDA **(f)** in distinguishing individuals with AD-related MCI (n = 52) from NCs (n = 47).

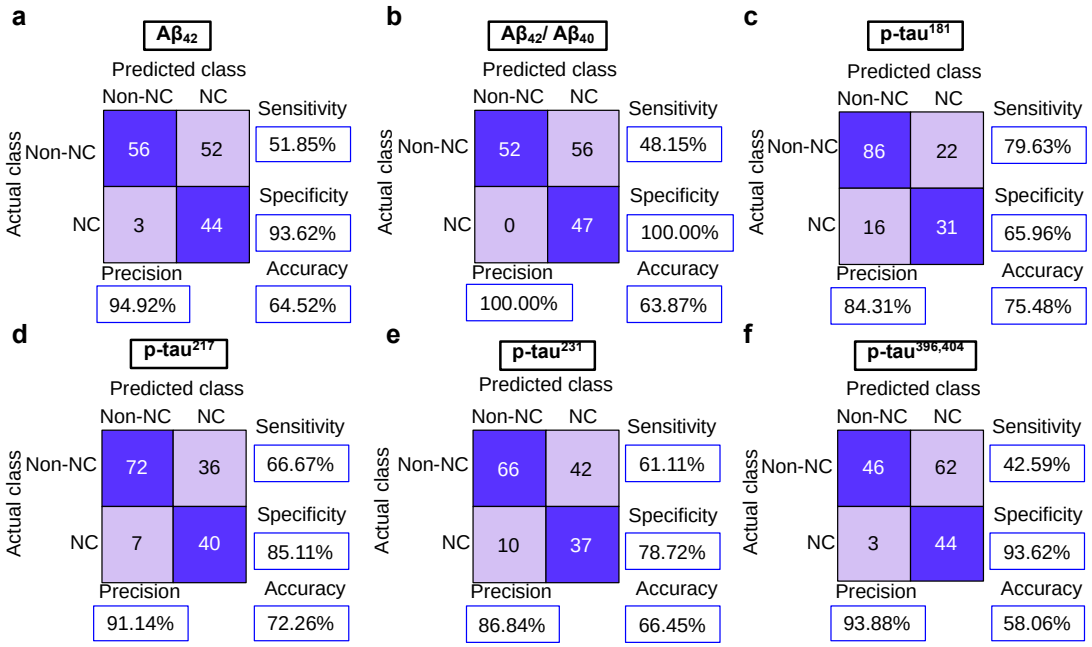

Supplementary Fig. 17 | Performance of UCMDA using a single biomarker in distinguishing non-NCs from NCs. a-f Sensitivity, specificity, precision, and accuracy of ROC analysis using the predictor of $A\beta_{42}$ **(a)**, $A\beta_{42}/A\beta_{40}$ ratio **(b)**, p-tau^{181} **(c)**, p-tau^{217} **(d)**, p-tau^{231} **(e)**, or p-tau^{396,404} **(f)** detected by UCMDA in distinguishing non-NCs (n = 108) from NCs (n = 47).

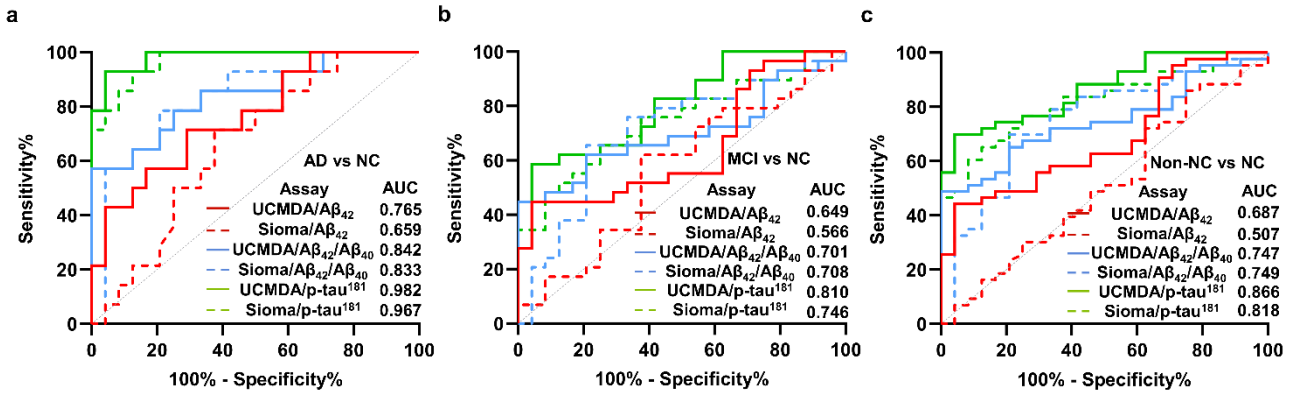

Supplementary Fig. 18 | ROC curves of UCMDA and Sioma for distinguishing AD, AD-related MCI, or non-NCs from NCs using the predictor of Aβ$_{42}$, Aβ$_{42}$/Aβ$_{40}$, or p-tau^{181}. a-c ROC curves of UCMDA and Sioma for distinguishing AD **(a)**, AD-related MCI **(b)**, and non-NCs from NCs **(c)** using the predictor of Aβ$_{42}$, Aβ$_{42}$/Aβ$_{40}$, or p-tau^{181}. (n = 14 for patients with AD, n = 29 for individuals with AD-related MCI, n = 24 for NCs, and n = 43 for non-NCs.)

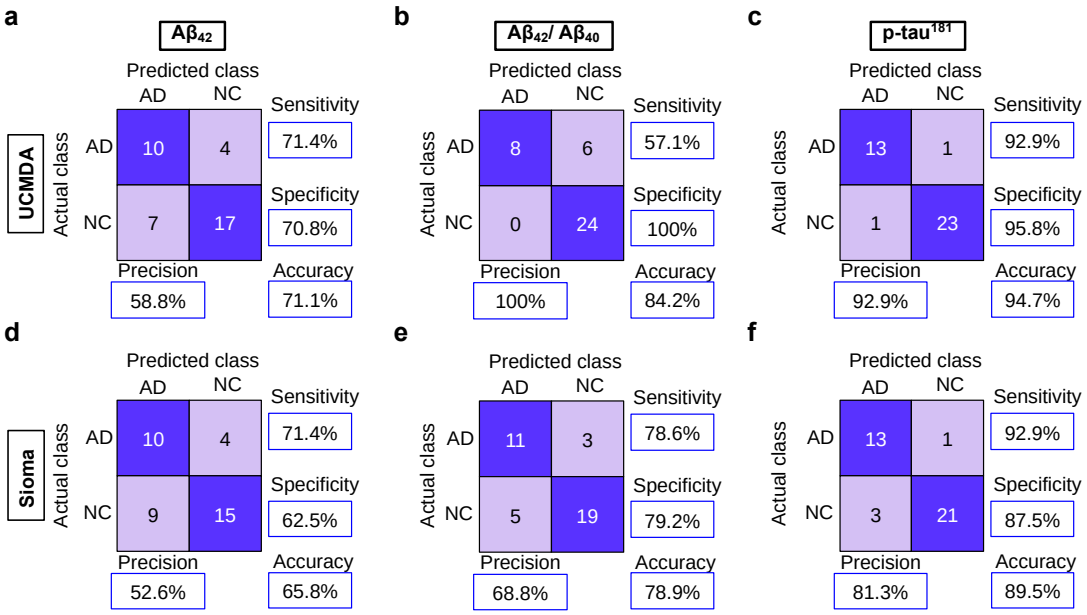

Supplementary Fig. 19 | Comparison of the performance of UCMDA and Sioma in distinguishing AD from NCs in the same clinical samples. a-f Comparison of the sensitivity, specificity, precision, and accuracy of UCMDA and Sioma in distinguishing AD (n = 14) from NCs (n = 24) using the predictor of $A\beta_{42}$ **(a, d)**, $A\beta_{42}/A\beta_{40}$ ratio **(b, e)**, or p-tau^{181} **(c, f)**.

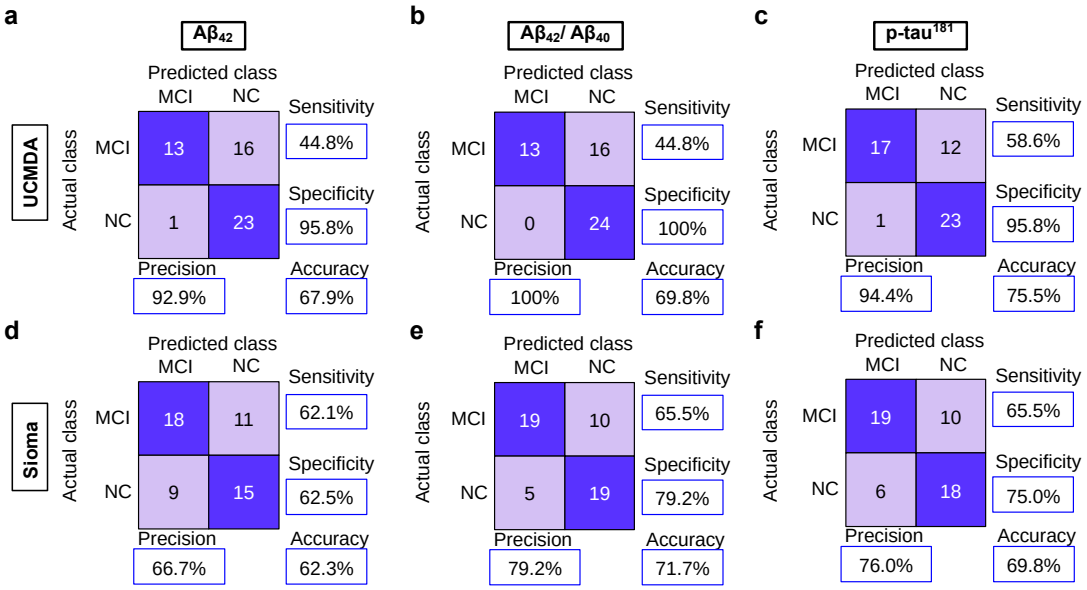

Supplementary Fig. 20 | Comparison of the performance of UCMDA and Sioma for distinguishing AD-related MCI from NCs in the same clinical samples. a-f Comparison of the sensitivity, specificity, precision, and accuracy of UCMDA and Sioma in distinguishing AD-related MCI (n = 29) from NCs (n = 24) using the predictor of $A\beta_{42}$ **(a, d)**, $A\beta_{42}/A\beta_{40}$ ratio **(b, e)**, or p-tau^{181} **(c, f)**.

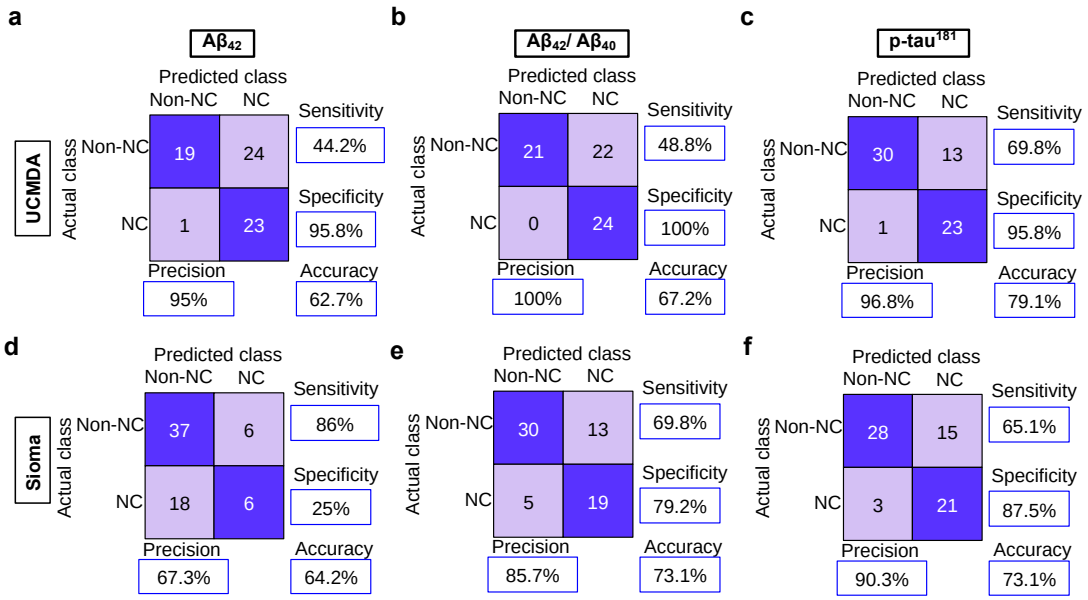

Supplementary Fig. 21 | Comparison of the performance of UCMDA and Sioma in distinguishing non-NCs from NCs in the same clinical samples. a-f Comparison of the sensitivity, specificity, precision, and accuracy of UCMDA and Sioma in distinguishing non-NCs (n = 43) from NCs (n = 24) using the predictor of $A\beta_{42}$ **(a, d)**, $A\beta_{42}/A\beta_{40}$ **(b, e)**, or p-tau^{181} **(c, f)**.

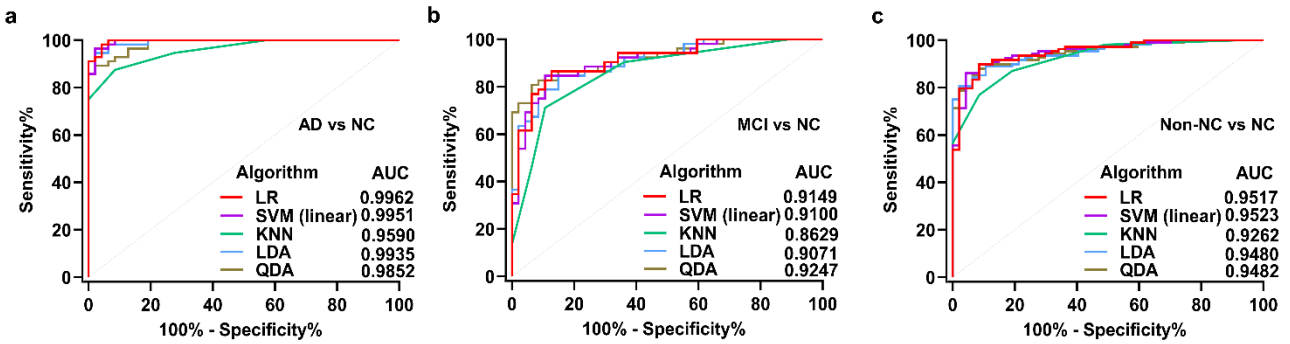

Supplementary Fig. 22 | ROC curves of different algorithms for distinguishing AD, MCI, or non-NCs from NCs. a-c ROC curves of LR, SVM (linear), KNN, LDA, or QDA algorithm based on the combination of six biomarkers for distinguishing AD **(a),** AD-related MCI **(b),** or non-NCs from NCs **(c)**. (n = 56 for patients with AD, n = 52 for individuals with AD-related MCI, n = 47 for NCs, and n = 108 for non-NCs.

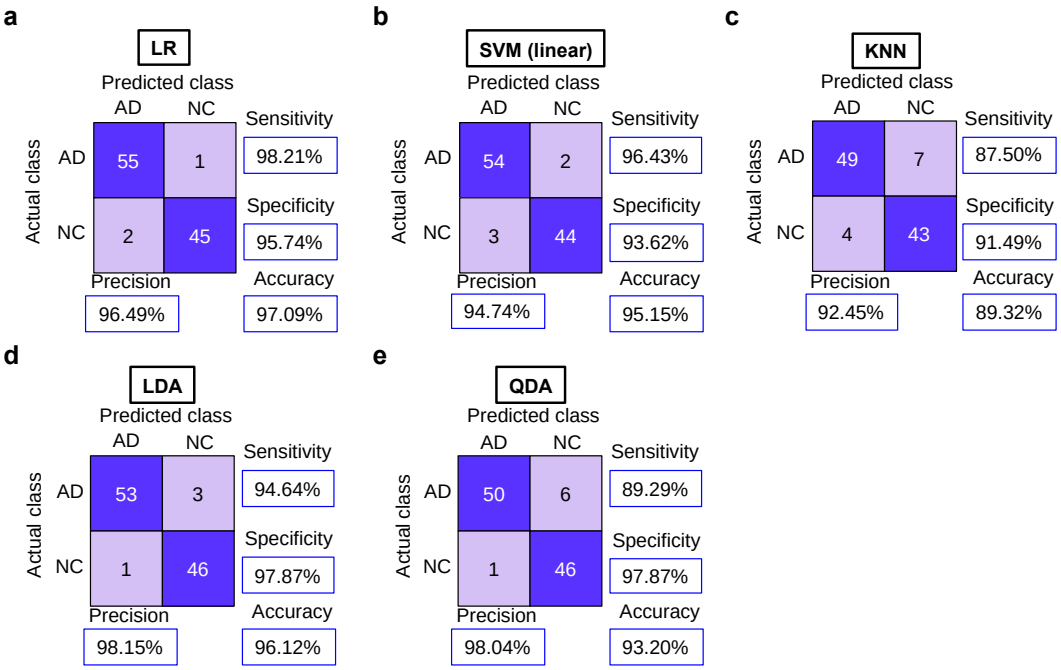

Supplementary Fig. 23 | Comparison of the performance of different algorithms in distinguishing AD from NCs. a-f Confusion matrix and corresponding metrics (sensitivity, specificity, precision, and accuracy) of ROC analysis based on the LR **(a)**, SVM (linear) **(b)**, KNN **(c)**, LDA **(d)**, or QDA **(e)** algorithm using the predictor of six biomarkers detected by UCMDA to distinguish patients with AD (n = 56) from NCs (n = 47).

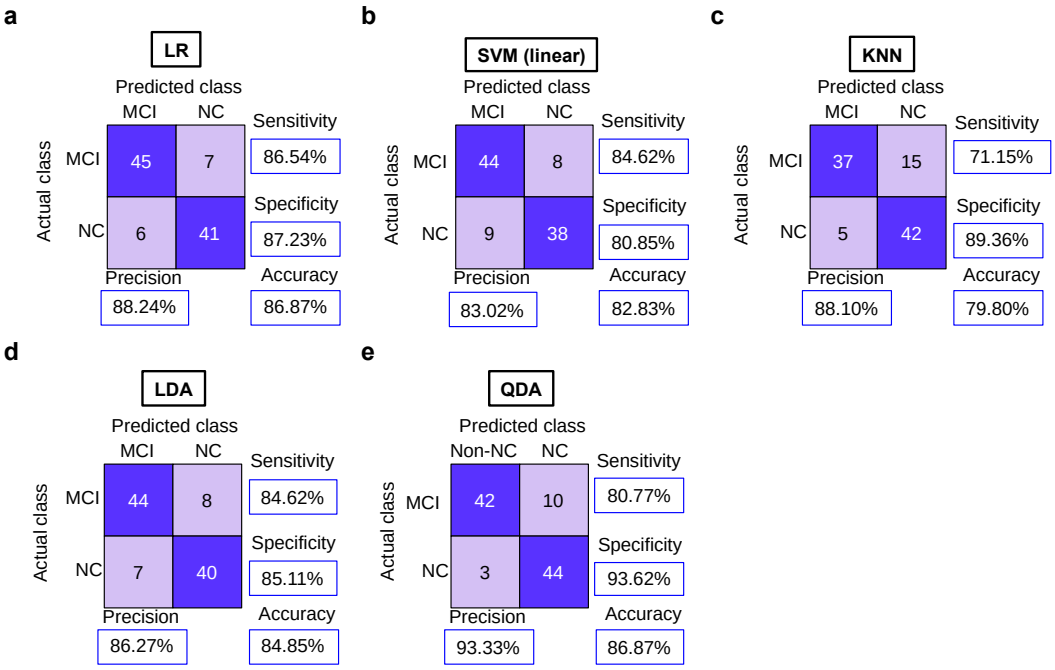

Supplementary Fig. 24 | Comparison of the performance of different algorithms in distinguishing AD-related MCI from NCs. a-f Confusion matrix and corresponding metrics (sensitivity, specificity, precision, and accuracy) of ROC analysis based on the LR **(a)**, SVM (linear) **(b)**, KNN **(c)**, LDA **(d)**, or QDA **(e)** algorithm using the predictor of six biomarkers detected by UCMDA to distinguish individuals with AD-related MCI (n = 52) from NCs (n = 47).

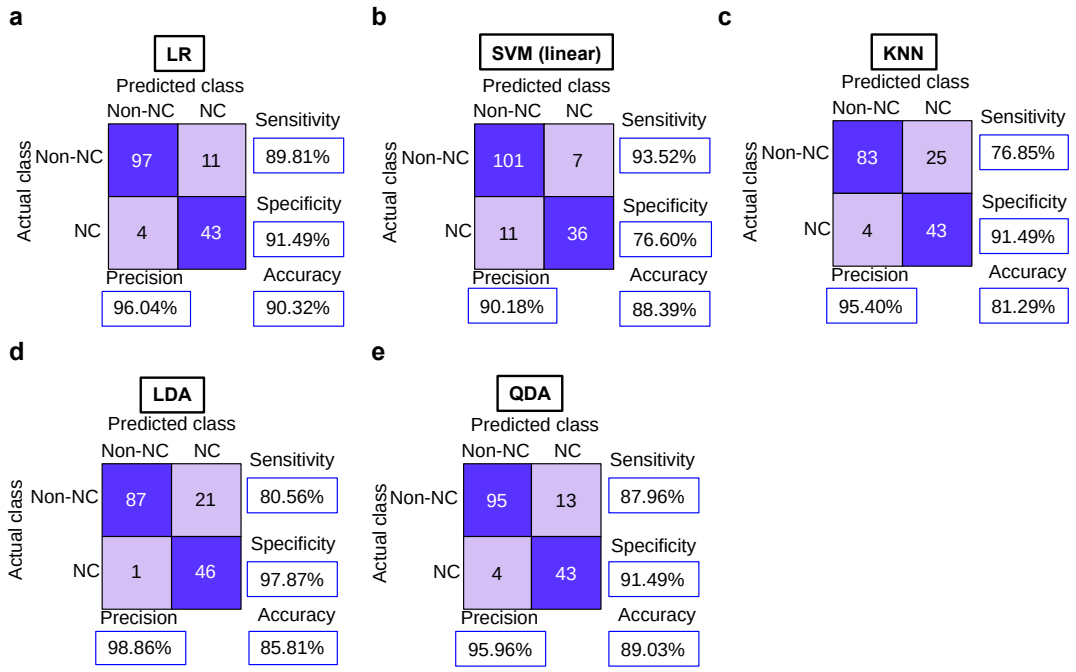

Supplementary Fig. 25 | Comparison of the performance of different algorithms in distinguishing non-NCs from NCs. a-f Confusion matrix and corresponding metrics (sensitivity, specificity, precision, and accuracy) of ROC analysis based on the LR **(a)**, SVM (linear) **(b)**, KNN **(c)**, LDA **(d)**, or QDA **(e)** algorithm using the predictor of six biomarkers detected by UCMDA to distinguish non-NCs (n = 108) from NCs (n = 47).

Supplementary Table 1 ssDNA sequences used in UCMDA

Name	Sequence (5'-3')
ssDNA 91	GGAGATTAGCAGTTTAGACTAAGAGTCCATTCCTCCCTCCTACTGCTATGGCTTAGGAAGTTCAGGTATAATTATGGGATCGTCATCGTTC
ssDNA 96	GCTACAAGGTTAATTAGGCAGTTACCAACCTGTTGAATACGCGCGTCTCCAGGTGCTTTTTCGTATGCTTTTGGTATAAGGCCAGAGGAATAATGC
ssDNA 97	CAACTTAAAGGGGGATGTGTAGACTAGAAATACTTTTGCTGTATCTACTTTGCGTAGCAGATTTCCCCGAAGCCCATAAAGTACTATGATCTCAGAC
ssDNA 99	GACATACGGTCTTAATAGACCAAAGATTCGTGAGCGTAGTCCTGGGGGCTCGCCTACCGTTTAAAATAACCCAAAGTATAATCAAGGGGAACGCTCAAC
ssDNA O102	CTATGCTGTAACTTTCCCGGATGATATTTATGCGGAGAGCAGTACTTCAGCGGATGCAGTAATTTCTGGTGACAATAACCCGGACCATAAACTGAAAGTTTC
ssDNA N102	CAGCGCAATAATCTGGTTACTTTTCCTCAATTTTCTGATAGAAACAATATCAGACAAAAGGAATATTATTTTCATTTTAATCAGATAACCACTCTTCCGGAG

Supplementary Table 2 RPA primer sequences used in UCMDA

Name	Sequence (5'-3')
ssDNA 91F	GGAGATTAGCAGTTTAGACTAAGAGTCCAT
ssDNA 91R	GAACGATGACGATCCCATAATTATACCTGA
ssDNA 96F	GCTACAAGGTTAATTAGGCAGTTACCAAC
ssDNA 96R	GCATTATTCCTCTGGCCTTATACCAAAAG
ssDNA 97F	CAACTTAAAGGGGGATGTGTAGACTAGAA
ssDNA 97R	GTCTGAGATCATAGTACTTTATGGGCTTC
ssDNA 99F	GACATACGGTCTTAATAGACCAAAGATTCG
ssDNA 99R	GTTGAGCGTTCCCCTTGATTATACTTTG
ssDNA O102F	CTATGCTGTAACTTTCCCGGATGATATTTA
ssDNA O102R	GAAACTTTCAGTTTATGGTCCGGGTTATT
ssDNA N102F	CAGCGCAATAATCTGGTTACTTTTCCTC
ssDNA N102R	CTCCGGAAGAGTGGTTATCTGATTAAAATG

Supplementary Table 3 crRNA sequences and the probe used in UCMDA

Name	Sequence (5'-3')
crRNA 91	GAAUUUCUACUGUUGUAGAUGACUAAGAGUCCAUUCCUCCCUCC
crRNA 96	GAAUUUCUACUGUUGUAGAUGUAUAAGGCCAGAGGAAUAAUGC
crRNA 97	GAAUUUCUACUGUUGUAGAUCCCGAAGCCCAUAAAGUACUAUGA
crRNA 99	GAAUUUCUACUGUUGUAGAUAAAUAACCCAAAGUAUAAUCAAGG
crRNA O102	GAAUUUCUACUGUUGUAGAUUGCGGAGAGCAGUACUUCAGCGGA
crRNA N102	GAAUUUCUACUGUUGUAGAUUGAUAGAAACAAUAUCAGACAAAA
Probe	FAM-TTTTTT-BQH

Supplementary Table 4 Comparison of UCMDA with other detection methods

Method	Analytes	LOD	AUC	Sample	Ref
UCMDA	$A\beta_{40}$,	1 fg/mL	0.595	plasma	This work
	$A\beta_{42}$,		0.787		
	p-tau^{181},		0.91		
	p-tau^{217},		0.82		
	p-tau^{231}		0.826		
	and p-tau^{396,404}		0.819		
ELISA	$A\beta_{42}$, tau, or p-tau^{181}	1.56 pg/mL	0.93, 0.89, 0.88	CSF and exosome	1
Paper-based lateral flow immunoassay	$A\beta_{42}$Ms and $A\beta_{42}$Os	154 pg/mL	NA	blood	2,3
	$A\beta_{40}$,	191.2 fg/mL		Buffer environment	
	$A\beta_{42}$,	138.1 fg/mL			
	tau,	257.1 fg/mL			
	and NfL	309.1 fg/mL			
Dual-mode magnetic immunosensor	p-tau^{396,404}	1.5 pg/mL	0.93	blood	4
SERS based immunoassay	p-tau^{396,404}	3.8 pg/mL	NA	plasma	5,6
	tau	1.21 pg/mL			
	$A\beta_{42}$	46.2 pg/mL			
Simoa	p-tau^{181}	9.31 pg/mL	0.77	plasma	7
MSD	p-tau^{181},	0.8 pg/mL	0.8	plasma	8
	p-tau^{217},	0.13 pg/mL	0.81		

	or p-tau^{231}	0.04 pg/mL	0.81		
	$A\beta_{40}$,		0.85		
Immunomagnetic	$A\beta_{42}$,		0.993	plasma and	
PCR	p-tau^{181},	10 fg/mL	0.79	exosome	9
	and p-tau^{396,404}		0.95		
	$A\beta_{40}$,	47.96 fg/mL	0.608		
Carbon	$A\beta_{42}$,	45.44 fg/mL	0.8		
nanotubes array	tau,	734.2 fg/mL	0.815	plasma	10
	and p-tau	1.0 pg/mL	0.87		

Supplementary Table 5 Demographic characteristics of the participants

Participant information	Normal senile control	Mild cognitive impairment	AD
Numbers	47	52	56
Male/Female	22/25	24/28	32/24
Ages	68 ± 6.1	69.8 ± 6.1	70 ± 7.3
MoCA score	26.4 ± 2.2	22.5 ± 2.6	12.9 ± 5.2
CDR	0	0.42 ± 0.2	1.2 ± 0.6
Aβ-PET positive/negative	0/47	17/35	56/0

Supplementary Table 6 AUC value, sensitivity, specificity, precision, and accuracy of ROC analysis based on UCMDA using the predictor of single biomarker in distinguishing between AD patients and NCs

Biomarker	AUC	Sensitivity (%)	Specificity (%)	Precision (%)	Accuracy (%)
$A\beta_{42}$	0.8514	66.07	89.36	88.10	76.70
$A\beta_{42}/A\beta_{40}$	0.8302	57.14	100.00	100.00	76.70
p-tau^{181}	0.8522	96.43	61.70	75.00	80.58
p-tau^{217}	0.9012	78.57	85.11	86.27	81.55
p-tau^{231}	0.8146	80.36	74.47	78.95	77.67
p-tau^{396,404}	0.7895	55.36	93.62	91.18	72.82

Supplementary Table 7 AUC value, sensitivity, specificity, precision, and accuracy of ROC analysis based on UCMDA using the predictor of the single biomarker in distinguishing between AD-related MCI and NCs

Biomarker	AUC	Sensitivity (%)	Specificity (%)	Precision (%)	Accuracy (%)
$A\beta_{42}$	0.6833	38.46	97.87	95.24	66.67
$A\beta_{42}/A\beta_{40}$	0.6391	38.46	100.00	100.00	67.68
p-tau^{181}	0.7295	53.85	82.98	77.78	67.68
p-tau^{217}	0.7390	50.00	89.36	83.87	68.69
p-tau^{231}	0.6809	34.62	95.74	90.00	63.64
p-tau^{396,404}	0.6653	48.08	76.60	69.44	61.62

Supplementary Table 8 AUC value, sensitivity, specificity, precision, and accuracy of ROC analysis based on UCMDA using the predictor of single biomarker in distinguishing between non-NCs and NCs

Biomarker	AUC	Sensitivity (%)	Specificity (%)	Precision (%)	Accuracy (%)
$A\beta_{42}$	0.7719	51.85	93.62	94.94	64.52
$A\beta_{42}/A\beta_{40}$	0.7382	48.15	100.00	100.00	63.87
p-tau^{181}	0.7931	79.63	65.96	84.31	75.48
p-tau^{217}	0.8231	66.67	85.11	91.14	72.26
p-tau^{231}	0.7502	61.11	78.72	86.84	66.45
p-tau^{396,404}	0.7297	42.59	93.62	93.88	58.06

Supplementary Table 9 Comparison of AUC value, sensitivity, specificity, precision, and accuracy of UCMDA and Sioma using the predictor of $A\beta_{42}$, $A\beta_{42}/A\beta_{40}$, or p-tau^{181} in distinguishing between AD patients and NCs

Methods	Biomarker	AUC	Sensitivity (%)	Specificity (%)	Precision (%)	Accuracy (%)
UCMDA	$A\beta_{42}$	0.765	71.4	70.8	58.8	71.1
	$A\beta_{42}/A\beta_{40}$	0.842	57.1	100	100	84.2
	p-tau^{181}	0.982	92.9	95.8	92.9	94.7
Sioma	$A\beta_{42}$	0.659	71.4	62.5	52.6	65.8
	$A\beta_{42}/A\beta_{40}$	0.833	78.6	79.2	68.8	78.9
	p-tau^{181}	0.967	92.9	87.5	81.3	89.5

Supplementary Table 10 Comparison of AUC value, sensitivity, specificity, precision, and accuracy of UCMDA and Sioma using the predictor of $A\beta_{42}$, $A\beta_{42}/A\beta_{40}$, or p-tau^{181} in distinguishing between AD-related MCI and NCs

Methods	Biomarker	AUC	Sensitivity (%)	Specificity (%)	Precision (%)	Accuracy (%)
UCMDA	$A\beta_{42}$	0.649	44.8	95.8	92.9	67.9
	$A\beta_{42}/A\beta_{40}$	0.701	44.8	100	100	69.8
	p-tau^{181}	0.810	58.6	95.8	94.41	75.5
Sioma	$A\beta_{42}$	0.566	71.4	62.5	52.6	65.8
	$A\beta_{42}/A\beta_{40}$	0.708	65.5	79.2	79.2	71.7
	p-tau^{181}	0.746	65.5	75.0	76.0	69.8

Supplementary Table 11 Comparison of AUC value, sensitivity, specificity, precision, and accuracy of UCMDA and Sioma using the predictor of $A\beta_{42}$, $A\beta_{42}/A\beta_{40}$, or p-tau^{181} in distinguishing between non-NCs and NCs

Methods	Biomarker	AUC	Sensitivity (%)	Specificity (%)	Precision (%)	Accuracy (%)
UCMDA	$A\beta_{42}$	0.687	44.2	95.8	95	62.7
	$A\beta_{42}/A\beta_{40}$	0.747	48.8	100	100	67.2
	p-tau^{181}	0.866	69.8	95.8	96.8	79.1
Sioma	$A\beta_{42}$	0.507	86.0	25.0	67.3	64.2
	$A\beta_{42}/A\beta_{40}$	0.749	69.8	79.2	85.7	73.1
	p-tau^{181}	0.818	65.1	87.5	90.3	73.1

Supplementary Table 12 The AUC value, sensitivity, specificity, precision, and accuracy of different algorithms using the predictor of composite biomarkers detected by UCMDA in distinguishing between AD patients and NCs

Algorithms	AUC	Sensitivity (%)	Specificity (%)	Precision (%)	Accuracy (%)
LR	0.9962	98.21	95.74	96.49	97.09
SVM (linear)	0.9951	96.43	93.62	94.74	95.15
KNN	0.9590	87.50	91.49	92.45	89.32
LDA	0.9935	94.64	97.87	98.15	96.12
QDA	0.9852	89.29	97.87	98.04	93.20

Supplementary Table 13 The AUC value, sensitivity, specificity, precision, and accuracy of different algorithms using the predictor of composite biomarkers detected by UCMDA in distinguishing between AD-related MCI and NCs

Algorithms	AUC	Sensitivity (%)	Specificity (%)	Precision (%)	Accuracy (%)
LR	0.9149	86.54	87.23	88.24	86.87
SVM (linear)	0.9100	84.62	80.85	83.02	82.83
KNN	0.8629	71.15	89.36	88.10	79.80
LDA	0.9071	84.62	85.11	86.27	84.85
QDA	0.9247	80.77	93.62	93.22	86.87

Supplementary Table 14 The AUC value, sensitivity, specificity, precision, and accuracy of different algorithms using the predictor of composite biomarkers detected by UCMDA in distinguish between non-NCs and NCs

Algorithms	AUC	Sensitivity (%)	Specificity (%)	Precision (%)	Accuracy (%)
LR	0.9517	89.81	91.49	96.04	90.32
SVM (linear)	0.9523	93.52	76.60	90.18	88.39
KNN	0.9262	76.85	91.49	95.40	81.29
LDA	0.9480	80.56	97.87	98.86	85.81
QDA	0.9482	87.96	91.49	95.96	89.03

Supplementary Table 15 Details of antibodies used in UCMDA platform

Antibody name	Target	Catalog number	Species	Source
A40	$A\beta_{40}$	V28704	Mouse	Commercial purchase
6E8	$A\beta_{42}$	V28702	Mouse	Commercial purchase
1F12	$A\beta_{42}$	1F12	Mouse	Laboratory preparation
2C6	$A\beta_{42}$	2C6	Mouse	Laboratory preparation
1E9	p-tau^{181}	1E9	Mouse	Laboratory preparation
1A2	p-tau^{217}	1A2	Mouse	Laboratory preparation
AT180	p-tau^{231}	MN1040	Mouse	Commercial purchase
4B1	p-tau^{396,404}	4B1	Mouse	Laboratory preparation

Supplementary Table 16 The sequence of synthesized peptides used in this study

Name	Sequence (N'-C')
$A\beta_{38}$	DAEFRHDSGYEVHHQKLVFFAEDVGSNKGAIIGLMVGG
$A\beta_{40}$	DAEFRHDSGYEVHHQKLVFFAEDVGSNKGAIIGLMVGGVV
$A\beta_{42}$	DAEFRHDSGYEVHHQKLVFFAEDVGSNKGAIIGLMVGGVVIA
p-tau^{181}	AKTPPAPK(p-T)PPSSGEP
p-tau^{217}	SRTPSLP(p-T)PPTREPK
p-tau^{231}	KVAVVR(p-T)PPKSPS
p-tau^{396,404}	RENAKAKTDHGAEIVYK(p-S)PVVSGDT(p-S)PRHL
p-tau$^{6-18-181}$	QEFEVMEDHAGTYGGGGSGGGGSGGGGSAKTPPAPK(p-T)PPSSGEP
p-tau$^{6-18-396,404}$	QEFEVMEDHAGTYGGGGSGGGGSGGGGSRENAKAKTDHGAEIVYK(p-S)PVVSGDT(p-S)PRHL

References

1. Jia, L. et al. Concordance between the assessment of Aβ42, T-tau, and P-T181-tau in peripheral blood neuronal-derived exosomes and cerebrospinal fluid. *Alzheimers Dement.* **15**, 1071-1080 (2019).

2. Zhang, L. et al. Quantitative assessment of AD markers using naked eyes: point-of-care testing with paper-based lateral flow immunoassay. *J. Nanobiotechnol.* **19**, 366 (2021).

3. Zhan, Y. et al. Ultrasensitive detection of multiple Alzheimer's disease biomarkers by SERS-LFA. *Analyst.* **147**, 4124-4131 (2022).

4. Zhang, L. et al. Colorimetric and surface-enhanced Raman scattering dual-mode magnetic immunosensor for ultrasensitive detection of blood phosphorylated tau in Alzheimer's disease. *Biosens. Bioelectron.* **222**, 114935 (2023).

5. Zhang, L. et al. Ultrasensitive and point-of-care detection of plasma phosphorylated tau in Alzheimer's disease using colorimetric and surface-enhanced Raman scattering dual-readout lateral flow assay. *Nano Res.* **16**, 7459-7469 (2023).

6. Zhang, X. et al. Robust and Universal SERS Sensing Platform for Multiplexed Detection of Alzheimer's Disease Core Biomarkers Using PAapt-AuNPs Conjugates. *ACS Sens.* **4**, 2140-2149 (2019).

7. Lleó, A. et al. Phosphorylated tau181 in plasma as a potential biomarker for Alzheimer's disease in adults with Down syndrome. *Nat. Commun.* **12**, 4304 (2021).

8. Mielke, M.M. et al. Comparison of Plasma Phosphorylated Tau Species With Amyloid and Tau Positron Emission Tomography, Neurodegeneration, Vascular Pathology, and Cognitive Outcomes. *JAMA Neurol.* **78**, 1108-1117 (2021).

9. Hu, S. et al. Sensitive detection of multiple blood biomarkers via immunomagnetic exosomal PCR for the diagnosis of Alzheimer's disease. *Sci. Adv.* **10**, eabm3088 (2024).

10. Kim, K. et al. Clinically accurate diagnosis of Alzheimer's disease via multiplexed sensing of core biomarkers in human plasma. *Nat. Commun.* **11**, 119 (2020).